



## Strathprints Institutional Repository

Keegan, Mark Hugh and Nash, David and Stack, Margaret (2013) *Numerical modelling of hailstone impact on the leading edge of a wind turbine blade*. In: EWEA Annual Wind Energy Event 2013, 2013-02-04 - 2013-02-07, Vienna.

Strathprints is designed to allow users to access the research output of the University of Strathclyde. Copyright © and Moral Rights for the papers on this site are retained by the individual authors and/or other copyright owners. You may not engage in further distribution of the material for any profitmaking activities or any commercial gain. You may freely distribute both the url (<http://strathprints.strath.ac.uk/>) and the content of this paper for research or study, educational, or not-for-profit purposes without prior permission or charge.

Any correspondence concerning this service should be sent to Strathprints administrator: <mailto:strathprints@strath.ac.uk>

# NUMERICAL MODELLING OF HAILSTONE IMPACT ON THE LEADING EDGE OF A WIND TURBINE BLADE

Mark Hugh Keegan  
Wind Energy Systems CDT,  
University of Strathclyde  
mark.h.keegan@strath.ac.uk

Prof. David Nash  
Mechanical & Aerospace  
Engineering,  
University of Strathclyde

Prof. Margaret Stack  
Mechanical & Aerospace  
Engineering  
University of Strathclyde

## Abstract

The scale of modern blades means that tip speeds in excess of  $100\text{ms}^{-1}$  are now common in utility scale turbines. Coupling this with a hailstone terminal velocity ranging from  $9\text{ms}^{-1}$  to  $40\text{ms}^{-1}$ , the relative impact velocity becomes highly significant. There is little published data on the performance of blade materials under these impact conditions and as such this work aims to understand the impact phenomena more clearly and consequently characterize the impact performance of the constitutive blade materials. To better understand hailstone impact, the LS-DYNA explicit dynamics code was employed to simulate hailstone impact on the blade leading edge. A Smooth Particle Hydrodynamics approach (SPH) was chosen to represent the hailstone geometry. It was found that the forces and stresses created during hail impact are significant and in some cases damaging, therefore posing both short and long term risks to the material integrity. It was also found that coating systems such as the gel coat provide essential – and in extreme conditions, sacrificial – protection to the composite substrate.

Keywords: Blades, Leading Edge, Hailstone, Impact, Composites

## 1. Introduction

As a result of increasing political, social and economic pressure and the requirements for sustainable energy sources, the demand for/and deployment of installed wind capacity has gone through an unprecedented increase.

As a result of a combination of factors such as planning issues and wind resource availability, many large wind farms are situated in environmentally hostile locations; such as offshore locations or mountainous/exposed terrains. In these environments the wind turbines are exposed to numerous environmental factors

such as: rain, ice, hailstones, extreme winds and lightning strikes. These inclement weather conditions combined with the vast and increasing scale of modern wind turbine designs present numerous unique engineering challenges. One such challenge is the threat posed by hailstone impact on the leading edge of a wind turbine blade, specifically at the blade tip region where the speeds are significant. Hailstone impact in this region presents a challenge with respect to the material technologies employed in the blade and their performance over the turbines lifespan (in many cases 25+ years).

This study evaluates the threat posed to the leading edge by hailstone impact through reviewing and evaluating the impact conditions and numerically simulating the impact phenomenon through the use of LS-DYNA software.

## 2. Hail Stone Impact on the Leading Edge

### 2.1 Hailstone Characteristics

Of all the possible forms of precipitation to which a wind turbine can be exposed to, hailstones (or hailstorms) may be considered the most potentially violent; in comparison to impact from rain, snow, sea-spray etc.

Hailstones can range in diameter from 5mm (the minimum size for hailstone classification) to in excess of 50mm in more extreme cases [1]. These large diameters also result in increased theoretical terminal velocities for hailstone, as described by Equation 1.

$$V_t = \sqrt{\frac{2m_h g}{C \rho_{air} A_h}} \quad \text{Eq. 1}$$

Where  $V_t$  is the terminal velocity,  $m_h$  is the mass of the hailstone,  $C$  is the drag coefficient of the hailstone,  $\rho_{air}$  is the air density and  $A_h$  is the cross sectional area of

the hailstone. This expression is derived through balancing the gravitational forces and drag forces acting on the hailstone when in free fall. It shows that with an increase in diameter the terminal velocity increases. It is this increased terminal velocity and increased projectile mass that presents a step change in impact energies when compared to rain droplet impact.

## 2.2 Frequency

As discussed, the potential ferocity of hailstone impact events either individually or collectively over time are what make them an important engineering consideration. However it is also apparent that the frequency of hailstone impact events when compared to that of rain is much lower and will be heavily dependent on both site location and climatic conditions.

It is possible though to assess the likelihood and frequency of hail impact events through examining meteorological data. For example, Figure 1 shows a map of the average annual total recorded days of hail in the UK for the period of 1971-2000

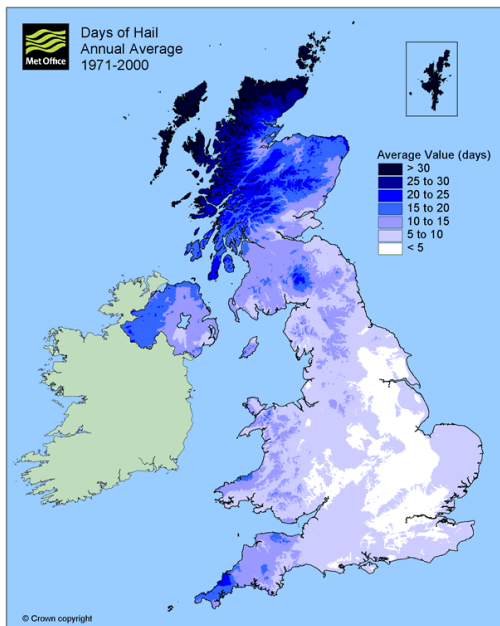


Figure 1: Days of Hail Annual Average 1971-2000, source: [2]

From this map it is clear to see that in some regions of the UK hailstones are commonplace with some areas around the North West of Scotland experiencing in excess of 30 days of hail on an annual basis; interestingly, areas of good wind

resource. However, it is also apparent that for other regions the frequency of hail storms is very low, highlighting the influence of site location on potential hailstorm exposure.

## 2.3 Impact Conditions

Through advancements in material technologies and structural design, the scale of modern utility scale wind turbine blades has increased dramatically in recent times. Through a combination of this increased scale and the operating requirements of modern wind turbines the tip speeds exhibited by blades has also increased greatly. Figure 2 shows a plot of the maximum tip speeds for a range of turbines from various manufacturers, plotted against their respective rotor diameter (generated from publically available turbine data). From the plot it is apparent that speeds in excess of  $80\text{ms}^{-1}$  are now common place, with many actually exhibiting tip speeds of about  $90\text{ms}^{-1}$  and some select designs exceeding  $100\text{ms}^{-1}$ .

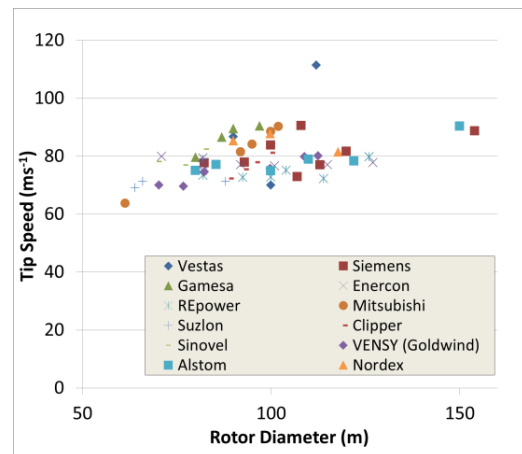


Figure 2: Wind Turbine Blade Tip Speed, source: numerous

However, the blade tip speed is only one influencing factor on the impact conditions at the leading edge of the blade. Two other important considerations are the terminal velocity of the hailstone and the incoming wind speed.

Through a simple velocity vector analysis, by taking the horizontal and vertical components of the blade tip tangential speed and combining them with the vertical (terminal) velocity of a given hailstone and the prevailing wind speed, it is possible to calculate the resultant theoretical maximum

impact speed on the blade for any given rotor position, hailstone size/mass and wind speed. For example, for a 20mm diameter hailstone with a density of  $900\text{kg/m}^3$  falling at its theoretical terminal velocity of  $19.6\text{ms}^{-1}$  (as given by Eq 1) striking the tip of a 45m long blade, rotating at  $1.8\text{rad/s}$  ( $81\text{ms}^{-1}$  tip speed), and assuming that the hailstone is fully entrained in a  $25\text{ms}^{-1}$  wind (i.e. matches its horizontal velocity), the impact velocity can be calculated through a full rotor sweep, as shown in Figure 3.

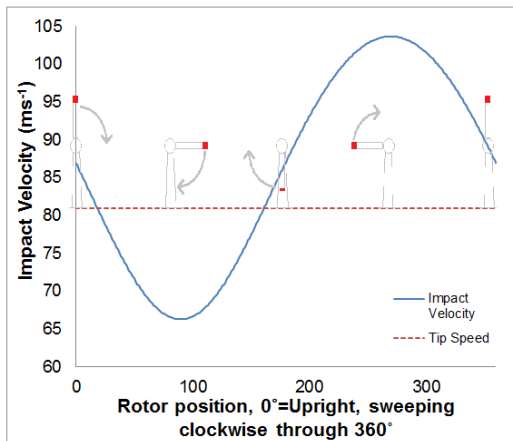


Figure 3: Impact velocity through a rotor sweep

From Figure 3 it is possible to see that for these hailstone conditions and blade length, impact velocities around and in excess of  $100\text{ms}^{-1}$  are feasible. As would be expected, the greatest impact velocity is created when the blade sweeps upwards and through the horizontal position ( $270^\circ$ ), where the tangential tip speed and terminal velocity of the hailstone act in opposite directions. It should also be noted that at this rotor position the load on the blade (and therefore stress in the blade material) will also be high due to the cantilever/free hanging condition. It can also be observed that even when the blade is swinging away from the direction of the hailstone fall, due to the high tip speed values, the possible impact velocities are still significant; never falling below  $65\text{ms}^{-1}$  in these conditions.

This analysis makes some simplifying assumptions, however it does give a clearer indication of the nature of impact on the leading edge of the wind turbine blade and the magnitude of the potential impact velocities.

## 2.4 Blade Materials

Modern utility scale wind turbines employ lightweight fiber reinforced plastic composite materials throughout the blade design. These materials possess the high specific strength and stiffness required to meet the structural criteria of the blade. However, some composite material technologies can be weak under impact and most are extremely sensitive to environmental factors such as heat, humidity, moisture and ice.

Most blade designs feature composites made from a thermosetting plastic (commonly epoxy or polyester) with either glass or carbon fiber reinforcement. However as stated, these technologies can be susceptible to damage through both impact and environmental exposure and consequently they require additional layers of protective coatings. Numerous coating technologies are available to address both impact protection and environmental protection. Coating technologies that offer impact protection are commonly referred to as Gelcoats. These can be applied in-mould if they are similar to the matrix material employed in the structural composites (epoxy, polyester etc.) or applied through spraying/painting once the blade is removed from the mould if the material is not compatible with the manufacturing process (polyurethanes).

In addition to the protective layers incorporated into the manufactured design, leading edge protection tape can also be applied, typically at sites where leading edge erosion is an issue; due to environment/climate. Unlike Gelcoats which are typically made of tough and stiff resins such as epoxy or polyester, leading edge tapes are typically made of polyurethanes which are more ductile and absorb impact energy through deformation.

## 3. Ice Impact Modelling

Hailstone impact events occur over fractions of a second and the mode of load transfer between the hailstone and the target body is highly dynamic. For these reasons it was deemed that a transient dynamic finite element analysis approach was required to model the impact phenomenon effectively.

There are numerous commercially available software packages for such analyses. However, one of the most commonly employed packages used for such high speed impact simulations is the LS-DYNA solver; widely utilised in aerospace and automotive studies. Additionally, much of the research and development of appropriate material models for ice has been conducted using LS-DYNA and the solver has a proven track record for capably modelling composite materials. It was for these reasons that LS-DYNA was chosen for the ice modelling work.

### 3.1 Ice Material Characteristics

Ice is a complex and highly variable material with regards to its material characteristics and properties and as such is widely considered as a class of material rather a single type. However, as hailstones form under ambient conditions they form as polycrystalline ice 1h, known as ordinary or terrestrial ice [3]. The density of ice - and hail ice in particular - is variable and depends on numerous factors such as the conditions of the weather system in which it was created. Ordinary ice is said to possess a density of  $917\text{kg/m}^3$  and this value increases somewhat with a decrease in temperature; however it cannot equal the density of liquid water [4]. Hailstones however, are usually found to possess a (sometimes considerably) smaller density when compared to ice and the recorded value can vary from site to site and from storm to storm.

Schulson [3] states that ice can exhibit two kinds of inelastic behaviour under compression. At low strain rates ice behaves in a ductile manner, but as the strain rate increases it begins to behave in a stiffer, brittle way. From Figure 4 it can be seen that as the strain rate increases the ice material begins to behave in a more brittle manner with a more linear stress-strain curve and decrease in post-yield deformation. The transition from ductile to brittle behaviour is reported to occur at a strain rate of the order of  $10^{-3}\text{s}^{-1}$ .

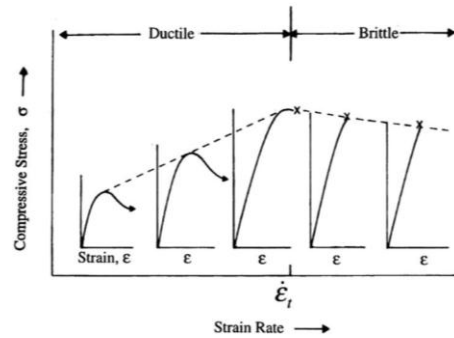


Figure 4 – Compressive behaviour of ice, source: [3]

This transition is an important consideration when attempting to model the material behaviour of ice, as it will experience dynamic and changing levels of strain rate during the impact event. It may also be expected that the strain rates imparted on the ice projectiles in the modelling work will reach values of up to and in excess of  $1000\text{s}^{-1}$ ; therefore any potential material models must also consider such strain rates.

### 3.2 Documented Ice Material Models

There have been a number of published attempts at modelling ice for the purposes of impact studies. Many studies attempt to account for the strain rate sensitivity of ice through tuning the material property inputs for specific impact conditions, such as the early model proposed by Kim et al. [5]. However, Carney et al. (2006) [6] proposed a material model for implementation in LS-DYNA (referred to hereafter as the Carney model) that incorporated the strain rate sensitivity through introducing a compressive stress scaling effect, relating to a range of possible strain rates. This in-built incorporation of strain rate sensitivity negates the need for tuning material properties for a given impact condition. In order to implement and evaluate the model, Carney et al. conducted a series of simulations to replicate impact tests carried out experimentally. The tests consisted of firing cylindrical ice projectiles, 42.16mm long and 17.46mm in diameter, at a rigid plate mounted on a force transducer measurement device, so that the impact force history for each test could be recorded.

As stated, the modelling work was performed using LS-DYNA. The target geometry was modelled using a classic Lagrangian meshing method (owing to its rigid configuration), however an Eulerian approach was adopted in order to mesh/model the ice projectile. This approach applies a mesh to a domain enclosing the geometry concerned, rather than applying the mesh to the geometry itself. This allows for large geometric deformations of the body concerned without skewing elements (as would be the case with a Lagrangian approach) which consequently increases computational time and/or results in a failure to solve. This approach is commonly employed where large deformations of the body concerned are predicted. In order to closely match the experimental conditions in the model, Carney et al. conducted a modal survey on the test apparatus. The results of the modal survey are shown in Figure 5.

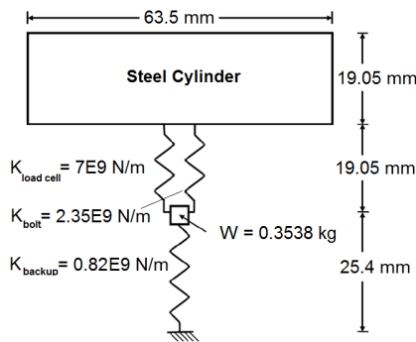


Figure 5: Modal survey results from Carney et al. (2006) [6]

This modal configuration was incorporated into the modelling work, which consisted of simulating impact at velocities of 91.44, 152.4 and 231.36ms<sup>-1</sup>, at angles of 0 and 45°. The force histories obtained for these conditions through the modelling efforts and the experimental work were then compared to successfully validate the material model developed.

Through reviewing all the appropriate ice material models in the literature, it was apparent that the material model proposed by Carney et al. represented the most developed and widely adopted model. For these reasons it was decided that this model would be adopted for the purposes of investigating hailstone impact on the leading edge of a wind turbine blade

### 3.3 Ice Modelling Methodology

Although an Eulerian approach to modelling high deformation impact events is commonly employed in modelling work (as in Carney et al. (2006) [6]), there is another meshless method named Smooth Particle Hydrodynamics (SPH). Anghileri et al. (2005) [7] conducted a survey of numerical approaches to model hailstone impact, comparing Lagrangian, Eulerian and SPH approaches; using ice material models that pre-date the work of Carney et al. (2006) [6]. The study found that the computational time required for a classic Lagrangian approach was great enough to discount it as a suitable modelling methodology. The results obtained for both the Eulerian and SPH approaches compared very closely both quantitatively and qualitatively. However the computational time required for the SPH approach was significantly less requiring only 1hr 4min compared to 14hr 30min for the Eulerian approach.

For these reasons it was decided that for the modelling work of this study an SPH approach would be employed. However, the Carney model was not originally developed using an SPH approach. Therefore, in order to both validate the compatibility of the ice material model with the SPH approach and also to ensure the model was implemented correctly, the modelling work detailed in the paper by Carney et al. [6] was replicated using the SPH approach; making it possible to then compare the results obtained and validate the method.

### 3.4 SPH Validation

For the purpose of setting up the analysis the LS-PrePost software package [8] was used. Due to the desired rigid behaviour of the target plate, (as in Carney et al. (2006) [6]) it was deemed suitable to model the plate through a classic Lagrangian mesh approach. Therefore the 63.5mm diameter, 19.05mm thick cylindrical plate geometry was created in LS-PrePost and was given a hexahedral mesh with a total of 5332, 8-noded solid hexahedral elements. As the target plate was to be considered as a rigid component, 'MAT\_RIGID' was used to represent the target plate material using the material properties of Type 304 Stainless Steel [9], shown in Table 1.



Table 1: Rigid plate material properties

Property	Value
Density (kg/m <sup>3</sup> )	8000
Young's Modulus (GPa)	193
Poissons Ratio	0.29

The particular elastic properties of the material used were not of any great importance as a result of modelling the plate as a rigid body; however the density would play a factor in adding a particular mass to the target apparatus.

In an attempt to match the modal characteristics of the target plate apparatus as discussed previously (and shown in Figure 5) three 'discrete' elements [10] were incorporated to the underside of the plate to represent the load cell, bolt and backup structure and fixed the 'ground'. The incorporation of this mass-spring system meant that the plate was only permitted to move in the plane of the spring elements during impact (the z-axis in the model) and all other degrees of freedom were constrained; these were the only boundary conditions applied to the model. As stated previously, the ice cylinder projectile was modelled using an SPH approach and was represented by approximately 50,000 SPH nodes, it was found through iteration that this amount gave a good balance between accuracy and computational time requirements.

The Carney model is implementable in LS-DYNA through its purpose made material model, 'MAT PLASTICITY COMPRESSION TENSION EOS'. The material properties for single crystal ice at -10°C, as detailed by Carney et al. (2006) [6] and shown in Table 2, were input to the model.

Table 2: Ice material properties, source: [6]

Property	Value
Density (kg·m <sup>-3</sup> )	897.6
Young's Modulus (GPa)	9.31
Poisson's Ratio	0.33
Initial compressive flow stress (MPa)	172.4
Initial tensile flow stress (MPa)	17.24
Plastic Tangent Modulus (MPa)	6.89
Pressure cut-off in compression (MPa)	4.93
Pressure cut-off in tension (MPa)	0.433

The material model also requires the input of the strain rate sensitivity behaviour of ice, this is accomplished through the input of the compressive stress scaling factor data shown in Table 3, also detailed by Carney et al. (2006) [6].

Table 3: Ice Strain Sensitivity, source: [6]

Strain Rate (s <sup>-1</sup> )	Stress Scale Factor
1	1
10	1.2566
100	1.5132
200	1.59044
300	1.63562
400	1.66768
500	1.69255
600	1.71287
700	1.73005
800	1.74493
900	1.75805
1000	1.76979
1100	1.78042
1500	1.81498
10000	2.02639

The final required inputs are the details of an equation of state named '\*EOS TABULATED COMPACTION' which describes the relationship between volumetric strain and pressure in the ice material, the input values are shown in Table 4.

Table 4: Equation of state for ice, source: [6]

In Volumetric Strain	Pressure	Bulk Modulus
0	0 MPa	8.96 GPa
-7.69 x 10 <sup>-3</sup>	68.9 MPa	8.96 GPa
-3.13 x 10 <sup>-2</sup>	68.9 MPa	2.2 GPa
-10	68.9 MPa	6.89 MPa

For the purpose of modelling the contact between the hailstone and the target plate the contact algorithm named '\*CONTACT AUTOMATIC NODES TO SURFACE' was implemented with the 'SOFT 1' formulation activated which enables better contact modelling between bodies with vastly varying stiffness (in our case ice and steel). Each simulation was set to run for 900µs in accordance with the cases presented in Carney et al. (2006) [6]. The time step was determined automatically by the software package for each simulation however a time step reduction factor of 0.5 was input in order to keep the time step small and therefore maintain an acceptable level of model stability/accuracy and contact modelling effectiveness. The model was set to the deformation force of the spring elements (load cell) during impact.

Figure 6 shows the development of the simulated ice impact at a velocity of 152.4ms<sup>-1</sup> obtained from the results of the SPH validation modelling.

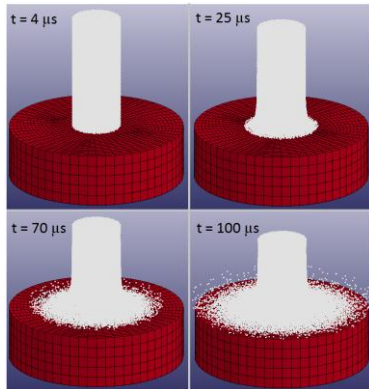


Figure 6: SPH ice projectile impact

Comparing this to the images from the paper by Carney et al. (2006) [6], shown in Figure 7, it can be said the attempts to replicate the modelling work have produced qualitatively comparable results. Both Figure 6 and Figure 7 show the ice structure breaking down from a solid to a fluid/powder-like consistency as the impact event develops.

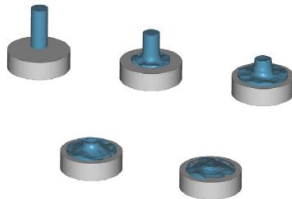


Figure 7: Eulerian ice projectile impact, source: [6]

Figure 8 shows the deformation force history plot of the discrete spring element representing the load cell during the SPH analysis (shown in red and labelled 'A') for an impact velocity of  $152.4\text{ms}^{-1}$  and compares them to the analytical and experimental results detailed by Carney et al. (2006) [6].

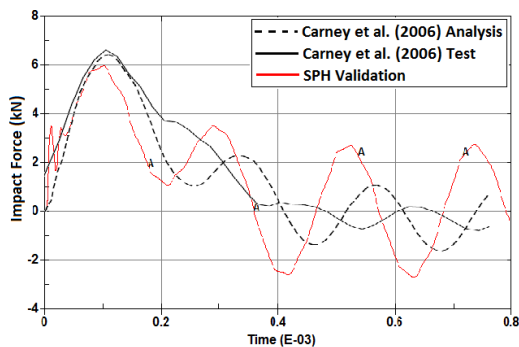


Figure 8: SPH approach force history results, plotted against results from Carney et al. (2006) [6]

From this plot it can be seen that the impact force history obtained through the SPH method implemented in this research compares well with the results obtained by Carney et al. (2006) [6]. This close comparison was also achieved at impact velocities of  $91.44$ , and  $231.36\text{ms}^{-1}$ . Through achieving both qualitatively and quantitatively comparable results to those detailed by Carney et al. (2005) [6], it was deemed that the SPH approach was a suitable and effective way to implement the Carney model in LS-DYNA.

## 4. Hailstone Leading Edge Impact

Through validating the SPH ice modelling approach against the results detailed by Carney et al. (2006) [6], it was then possible to further utilise this ice modelling approach to look at the effects of hailstone impact on the leading edge of a wind turbine blade component.

### 4.1 Leading Edge Geometry

Through personal communication with a large wind turbine blade manufacturer it was possible to obtain the geometry of a leading edge profile and the material layup configuration; described as typical of a real wind turbine blade leading edge tip. The geometry as provided is shown in Figure 9.

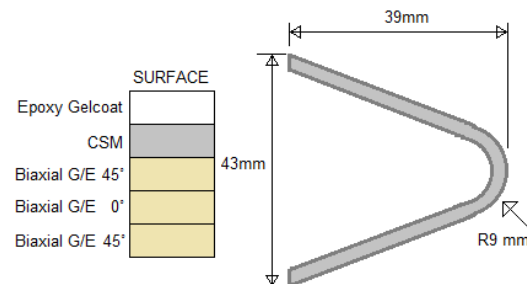


Figure 9: Blade leading edge geometry & Layup

LS-PrePost was again used to create this geometry and also to mesh the geometry. The layup configuration of the laminate created is also shown, comprising of an epoxy gelcoat layer, an epoxy/glass Chopped Stand Mat layer (CSM) and three layers of biaxial glass/epoxy composite; each layer was created with a thickness of  $400\text{microns}$ . Care had to be taken when meshing the composite layers to ensure that the material axes in the elements were orientated in the correct direction (i.e. the



direction of the layup configuration). The material properties (and chosen material models) of the two protective layers are given in Table 5.

Table 5 – Material properties of protective layers

Material	Epoxy Gelcoat	CSM
Source	Various	Various
Density	1400	1100
Young's Modulus (GPa)	7	3.5
Poissons Ratio	0.33	0.33
Tensile Strength (MPa)	80	65
Elongation at break (%)	1.6	3
LS-DYNA Material Model	MAT_003	MAT_003

These properties were ascertained through various sources and are deemed only an approximate representation of the typical material properties. Future work will look to find more definitive material properties through working with industrial contacts.

Table 6 details the material properties of the biaxial epoxy/glass composite layers. These values were taken from a paper by Menna et al. (2011) [11] and are based on a composite with a plain-weave E-Glass fabric, 295g/m<sup>2</sup> in areal weight, in a Cycom 7701 epoxy resin. These values were chosen both because the areal weight was close to that as specified by the blade manufacturer and due to the completeness of the material data supplied in the source; especially with regards to the interlaminar strength. As with in the study by Menna et al. (2011) [11] the material model selected for these composite layers was 'MAT COMPOSITE FAILURE SOLID MODEL'. The contact between layers of the laminate were set by the LS-DYNA contact algorithm, named 'CONTACT AUTOMATIC SURFACE TO SURFACE TIE-BREAK' and the values for interlaminar strength detailed in Table 6 were applied between all layers. Option 5 in the contact algorithm was

chosen to model delamination.

To allow for the effect of erosion in each layer the 'MAT ADD EROSION' tool was utilised, which removes elements from the model upon reaching a certain failure criteria. For the purposes of this work, the criterion was specified as the strain failure value for each specific material.

As stated, the material properties used come from either literature or through judgment based on material manufacturer data. It is hoped that in future modelling work – through interaction with blade and material manufacturers - actual blade material data will be available for input and study. However, for preliminary analysis and to test and evaluate the capabilities of LS-DYNA for this type of study, the material data used serves as a good approximate for a real blade leading edge.

## 4.2 Impact Conditions

It was decided that for the initial modelling work direct-normal impact on the blade leading edge would be investigated. To evaluate the effects of hailstone size and impact energy, three hailstone diameters of 5, 10 and 15 were modelled at impact velocities ranging from 70-120ms<sup>-1</sup> (in 10ms<sup>-1</sup> increments).

The material properties for ice as used in the previous SPH validation study were again implemented. As discussed previously, hailstone ice material properties can differ greatly from that of manufactured ice. However, for the preliminary purposes of evaluating the LS-DYNA modelling approach discussed for the purposes of simulating hailstone impact, this approach was deemed suitable. Symmetry boundary conditions were applied to the edges of the blade profile and the ends of the blade were

Table 6 – Material properties for composite layers, source: [11]

Orientation	Young's Modulus (GPa)	Tensile Strength (MPa)	Compressive Strength (MPa)
1	26	414	458
2	26	414	458
3	8	120	500
	Shear Modulus (GPa)	Shear Strength (MPa)	Poissons Ratio
12	3.8	105	0.1
23	2.8	65	0.25
13	2.8	65	0.25
	Interlaminar Normal Failure Stress (MPa)	Interlaminar Shear Failure Stress (MPa)	Strain Failure (%)
	35	65	1.81

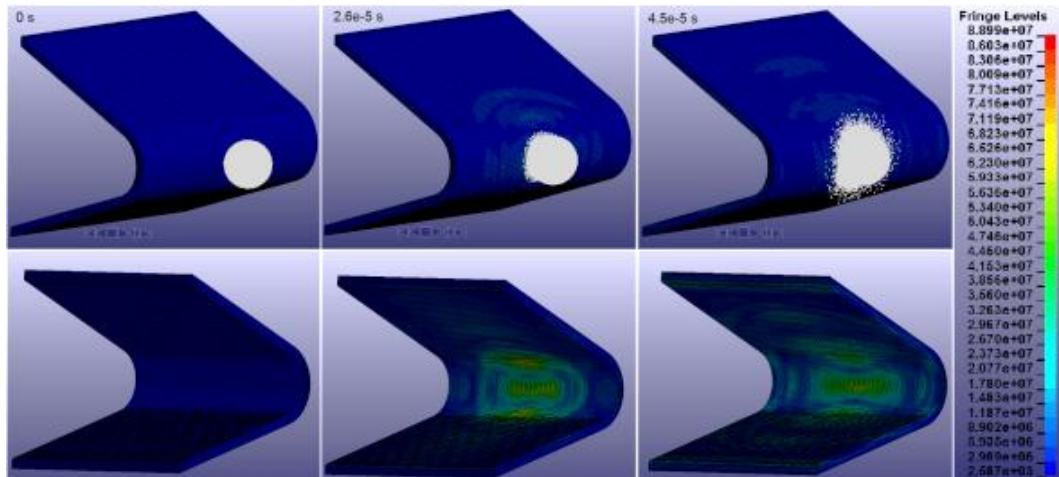


Figure 10: 10mm diameter hailstone impact at  $100\text{ms}^{-1}$ , contours of von-Mises Stress

constrained in the direction of the impact.

It is also prudent to note that no pre-stress was applied to the blade geometry during the modelling work, however in future work this may be included. The influence of pre-stress may play an important factor when considering that the horizontal blade position in which the maximum theoretical impact velocity occurs (Figure 3) is also a position in which large bending stresses in blade may be expected.

### 4.3 Results & Discussion

Figure 10 shows the progression of the modelled impact of a 10mm diameter hailstone at velocity of  $100\text{ms}^{-1}$ , showing contours of von-Mises stress in the blade materials. The images in the top row show the modelled hailstone impacting on the leading edge, and the bottom row shows the inner surface of the leading edge profile during the same impact (and same time steps).

From the plot the maximum stress is shown to be approximately 80MPa. Although this is not significant enough to cause failure in the composite substrate material itself (according to values in Table 6), it is sizeable enough to cause potential delamination across the laminate interfaces and potentially damage the protective layers. It is also possible to observe that the energy from the hailstone impact is absorbed throughout the thickness of the blade section, rather than just the upper layers; with significant stresses created in the lower layers (i.e. the composite substrate). This through thickness stress

absorption behaviour may mean that when considering hailstone impact damage, the areas affected may not be limited to the upper layers only. With regards to the possible types of damage creation, this sub-laminate stress distribution could result in many forms of material failure such as delamination between the layers or general material failure (e.g. tensile/compressive yield, fatigue). This type of substrate damage makes confidently assessing blade integrity/damage through only visual inspection problematic.

Figure 11 shows the maximum von-Mises Stress in the plate materials (all layers) during all of the simulation work performed. As can be seen, significant levels of stress can be created through impact from moderately sized hailstones. Given that the yield strengths of the Gelcoat and CSM layers are 80 and 65MPa respectively, the stresses can be considered damaging to the protective layers in many of the cases.

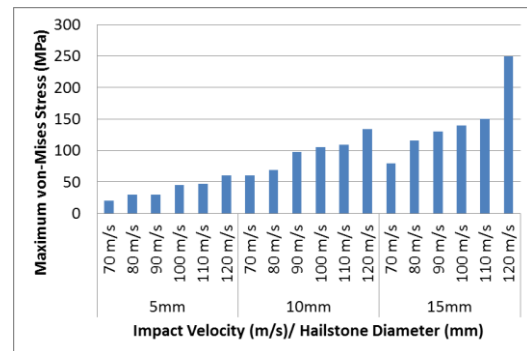


Figure 11: Maximum impact stress across hailstone diameters and velocities

With the inclusion of erosion in the modelling work it was also possible to investigate the occurrence of instantaneous leading edge damage through hailstone impact. For instance, Figure 12 shows the leading edge of the profile after the impact of a 15mm diameter hailstone at  $100\text{ms}^{-1}$ .

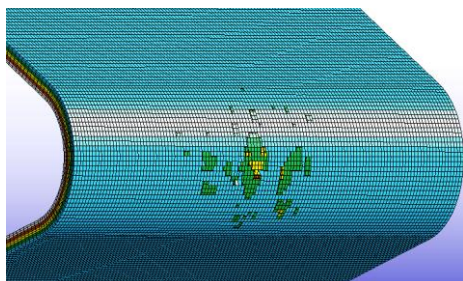


Figure 12: Results from erosion prediction, 15mm diameter hailstone at  $100\text{ms}^{-1}$  impact

As shown in Figure 12 (and predicted by the stress levels presented previously in Figure 11), leading edge erosion in the modelling work has occurred, evident by the removal of material from the upper layers, namely the gelcoat and CSM layers (but also to a lesser degree the first composite layer). This capability to model erosion is another powerful tool when considering blade design and when making decisions about leading edge protection. Given the right material data, it should be possible to also incorporate leading edge tape components into the model, to assess their performance and behaviour under impact

#### 4.4 Future Work

Through the work of identifying an appropriate material model and approach (SPH) with which to model ice/hailstone impact and establishing a typical leading edge profile baseline, the foundations for further and more comprehensive modelling work have been established. In order to gain confidence in the results obtained through the modelling work (both presently and in the future) and in turn increase the usefulness of the modelling work, there are two further actions required in future:

1. Obtain accurate and representative material properties for wind turbine blade technologies.
2. Conduct experimental hailstone impact analyses to obtain data with regards to stress and strain during impact, impact force and damage created. A hailstone

impact rig is currently under construction within the University of Strathclyde which will be used to conduct a wide range of hailstone impact tests to provide modelling validation.

It is hoped that through these actions, the results obtained through modelling can be validated, therefore extending the usefulness of the approach and the potential avenues of further research in relation to blade leading edge design.

## 5. Conclusions

The work so far has looked to review the issue of hailstone impact on the leading edge of wind turbine blades and identified the potential impact velocities as a plausible threat to the material integrity of the blade materials. In order to understand the phenomenon of hailstone impact on the leading edge it was decided that modelling work should be performed. The research then looked at establishing a suitable material model with which to model ice in the LS-DYNA modelling environment. Having chosen a suitable material model, that was also compatible with the SPH approach, preliminary blade impact studies were conducted. This exercise proved the worth of such an approach with respect to blade design and material performance assessment. The plans for future development of the model, in parallel with experimental validation efforts have also been detailed.

## References

- [1] Met Office, "National Meteorological Library and Archive Fact Sheet - Water in the Atmosphere," Devon, 2012.
- [2] Met Office UK, Last Accessed: Sept 2012. [Online]. Available: <http://www.metoffice.gov.uk/climate/uk/averages/ukmapavg.html>.
- [3] E. M. Schulson, "Brittle failure of ice," *Engineering Fracture Mechanics*, vol. 68, pp. 1839-1887, 2001.
- [4] R. C. Schroeder and W. H. McMaster, "Shock-compression freezing and melting of water and ice," *Journal of Applied Physics*, vol. 44, pp. 2591-4, 1973.
- [5] H. Kim and K. T. Kedward, "Modelling Hail Ice Impact and Predicting Impact Damage Initiation in Composite Structures," *AIAA Journal*, vol. 38, no. 7, pp. 1278-1288, July 2000.
- [6] K. S. Carney, D. J. Benson, P. DuBois and R. Lee, "A phenomenological high strain rate model with failure for ice," *International Journal of Solids and Structures*, vol. 43, pp. 7820-7839, 2006.
- [7] M. Anghileri, L. M. L. Castelleti, F. Invernizzi and M. Mascheroni, "A survey of numerical models for hail impact analysis using explicit finite element codes," *International Journal of Impact Engineering*, vol. 31, pp. 929-944, October 2005.

- [8] Livermore Software Technology Company, 2011. [Online]. Available: <http://www.lstc.com/corporate/profile>.
- [9] ASM Aerospace Specification Metals Inc., Last accessed Sept 2012. [Online]. Available: <http://asm.matweb.com/search/SpecificMaterial.asp?bassnum=MQ304A>.
- [10] Livermore Software Technology Corporation, *LS-DYNA Keyword User's Manual - Volume II Material Models*, 2012.
- [11] C. Menna, D. Asprone, G. Caprino, V. Lopresto and A. Prota, "Numerical simulation of impact tests on GFRP composite laminates," *International Journal of Impact Engineering*, vol. 38, no. 8-9, pp. 667-685, August-September 2011.